Journal of Alloys and Compounds 509 (2011) 9178–9182

Contents lists available at ScienceDirect

Journal of Alloys and Compounds

journal homepage: www.elsevier.com/locate/jallcom

# First-principles study on the electronic and optical properties of F- and Nb-doped anatase $TiO_2$

Rui-Shuo Zhang[a], Yong Liu[a,b], Qian Gao[a], Fan Teng[a], Chen-Lu Song[a,*], Wei Wang[c], Gao-Rong Han[a]

[a] State Key Laboratory of Silicon Materials, Department of Materials Science and Engineering, Zhejiang University, Hangzhou 310027, China
[b] Angstrom Center, Institute of Inorganic and Nonmetal Materials, Zhejiang University, Hangzhou 310027, China
[c] Weihai China Glass Solar Co., Ltd., Weihai 264205, China

ARTICLE INFO

*Article history:*
Received 7 April 2011
Received in revised form 24 June 2011
Accepted 24 June 2011
Available online 1 July 2011

*Keywords:*
Anatase $TiO_2$
First-principles
Electronic properties
Optical properties

ABSTRACT

We present a comparative study on the electronic and optical properties of Nb- and F- doped anatase $TiO_2$ by first-principles calculations based on the density functional theory (DFT). Although both $TiO_2$:Nb and $TiO_2$:F have a similar band structure, the effective mass of $TiO_2$:F is larger than that of $TiO_2$:Nb, and the carriers density in the former is lower than that in the latter, indicating that $TiO_2$:Nb has better electronic conductivity than $TiO_2$:F. The interaction between photons and electrons in $TiO_2$:F is much stronger than that in $TiO_2$:Nb, resulting in increased photon absorption and reduced transmittance, especially in the visible and near-infrared regions. The results demonstrate that $TiO_2$:F is not suitable for transparent conductive oxide applications.



## 1. Introduction

In the past several decades, transparent conductive oxides (TCOs) films have attracted much attention in research for their wide applications in solar cells, flat-panel displays (FPD) and light-emitting diodes (LED) [1,2]. And much efforts have been made in searching for new TCOs composed of more abundant elements to replace $In_2O_3$:Sn (ITO), which is one of the most popular TCOs now, for the scarcity of In element. Although ZnO:Al (AZO) and $SnO_2$:F (FTO) are thought to be promising TCOs that can replace ITO [3–5], the requirement for new TCOs remains because of the industrial demands for high-efficiency optoelectronic devices. In 2005, epitaxial thin films with Nb-doped anatase $TiO_2$ have been reported to be excellent TCOs with an electrical resistivity ($\rho$) of $2–3 \times 10^{-4}\,\Omega$ cm and an internal transmittance of about 95% in the visible region [6], which motivated intensive studies on TCOs based on anatase $TiO_2$, namely $Ti_{1-x}M_xO_2$ (M = Nb, Ta, W) [7–10], for its high refractive index, high transmittance in the infrared region and high chemical stability especially in a reducing atmosphere [11].

Given that nonmetal-doped $TiO_2$, such as $TiO_2$:F (N, S), is more thermally stable and less cost than metal-doped $TiO_2$ [12], and the doping of F element to substitute O is expected to release one extra electron and, possibly, result in $TiO_2$ products that have the similar electronic transport properties to $TiO_2$:Nb, F-doped anatase $TiO_2$ may provide another more promising TCO. Most of the previous studies, however, focused on the photocatalytic properties of the material, and paid less attention to its transport properties [13–16]. Despite several theoretical efforts have clarified the conducting properties of $TiO_2$:Nb to some extent, still little attention was paid to its transparent mechanisms [17–20].

In the present study, we investigate the electronic and optical properties of Nb- and F-doped anatase $TiO_2$ using first-principles calculations. Comparisons made between them demonstrate that F-doped anatase $TiO_2$ is not suitable for being utilized as a TCO material. The corresponding properties of undoped $TiO_2$ are also calculated as a reference.

## 2. Models and method of calculation

The calculations were carried out using the Cambridge Serial Total Energy Package (CASTEP) code. This code is based on the density functional theory (DFT), which uses a total-energy plane-wave pseudopotential method [21,22]. The exchange-correlation effects were treated within the generalized gradient approximation (GGA) with the Perdew–Burke–Ernzerhof (PBE) function [23]. The interaction between the valence electrons and the ionic core was modeled by norm-conserving

* Corresponding author. Tel.: +86 0 571 87951842; fax: +86 0 571 87951842.
*E-mail address:* songcl@zju.edu.cn (C.-L. Song).

0925-8388/$ – see front matter © 2011 Elsevier B.V. All rights reserved.
doi:10.1016/j.jallcom.2011.06.105

pseudopotentials with an energy cutoff of 550 eV, which is more suitable than ultra-soft pseudopotentials in the optical property calculations [24].

In the calculations, we simulated the anatase $TiO_2$ using a $2 \times 2 \times 1$ (48 atoms) supercell, where one Ti atom was replaced by Nb and one O atom was replaced by F to produce $TiO_2$:Nb and $TiO_2$:F, respectively (Fig. 1). The Monkhorst-Pack scheme *k*-point grid sampling was set to $3 \times 3 \times 3$ for the Brillouin zone in all calculations [25]. During geometry optimization, the parameters were set as follows: total energy tolerance = $5 \times 10^{-6}$ eV/atom, maximum force = 0.01 eV/Å, maximum stress = 0.02 GPa, and maximum displacement = $5 \times 10^{-4}$ Å. In addition, the empty bands, which are important in the calculations, especially for the optical properties, were increased to 20. These parameters were tested, and showed enough convergence for the energy calculation. After optimization, the band structure, density of states (DOS), electron density, Mulliken population and optical properties were calculated.

## 3. Results and discussion

### 3.1. Electronic properties

The band structure and DOS for $TiO_2$:Nb and $TiO_2$:F are shown in Fig. 2. From the first view, no impurity states are found in the band gaps for both. The Fermi levels of $TiO_2$:Nb and $TiO_2$:F enter into the conduction band, which is an indication that both are degenerated semiconductors. Thus, the Burstein-moss effect [26,27], which has been experimentally observed in $TiO_2$:Nb [28], can be predicted.

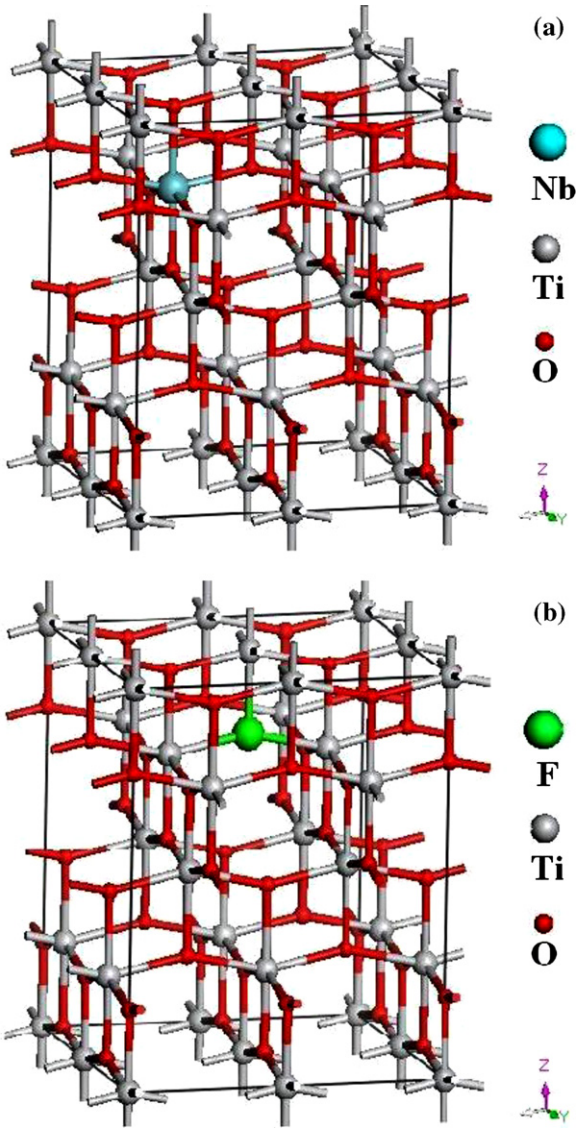


**Fig. 1.** Crystal structure of (a) Nb and (b) F doped anatase $TiO_2$.

$TiO_2$:Nb and $TiO_2$:F also have similar band gaps and valance band widths, and both show slightly larger than that of undoped $TiO_2$ (Table 1). The evaluated band gap of undoped $TiO_2$ is somewhat narrower than the empirical value (~3.2 eV for anatase $TiO_2$) [29], but is consistent with the calculations of Liu and his coworkers [18] using the local-density approximation (LDA) function (~2.12 eV). This underestimation is a well-known limitation of the DFT, but

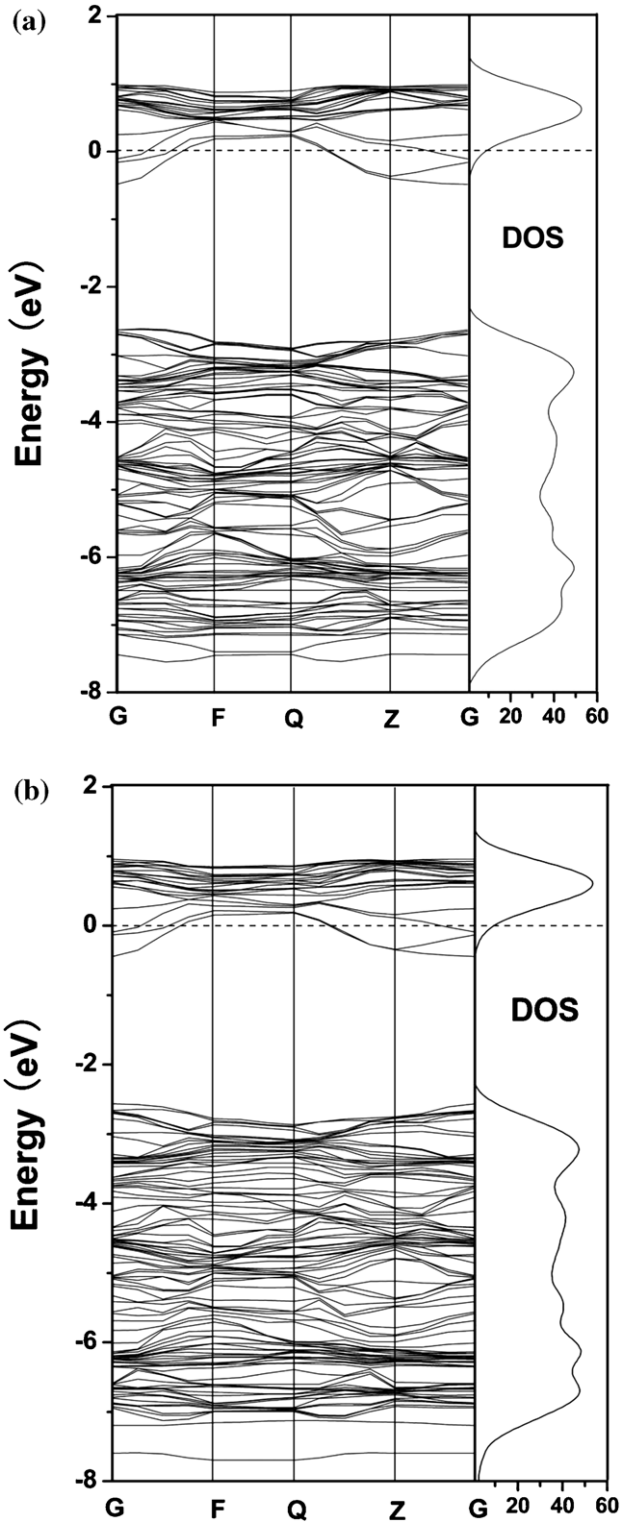


**Fig. 2.** Band structure and DOS for (a) $TiO_2$:Nb and (b) $TiO_2$:F. The horizontal dash line in both (a) and (b) indicate the Fermi level.

**Table 1**
Band gap, valance band width and effective mass for undoped anatase $TiO_2$, $TiO_2$:Nb and $TiO_2$:F ($m_0$ is the free electron mass).

| | | Undoped $TiO_2$ | $TiO_2$:Nb | $TiO_2$:F |
|---|---|---|---|---|
| Band gap (eV) | | 2.07 | 2.16 | 2.12 |
| Valance width (eV) | | 4.37 | 4.93 | 5.13 |
| $m_n^*/m_0$ | $a(b)$-axis | 0.53 | 0.53 | 0.62 |
| | $c$-axis | 4.20 | 4.11 | 4.29 |

will not affect the results' relative accuracy [30]. The similar band structure and DOS imply that $TiO_2$:F may have similar electronic conductivity with $TiO_2$:Nb.

From the band structure, we can also deduce the effective mass of carriers at the bottom of the conduction band using the following equation,

$$\frac{1}{m_n^*} = \frac{1}{\hbar^2}\frac{d^2E(k)}{dk^2} \quad (1)$$

where $m_n^*$ is the effective mass, $\hbar$ is the reduced Planck constant, and $E(k)$ is the wavefunction at $k$. The conduction band in the vicinity of the extrema is assumed to be parabolic, hence, the effective mass will be constant in these areas. The values of the calculated $m_n^*$ are also shown in Table 1. Apparently, the $m_n^*$ for undoped $TiO_2$, $TiO_2$:Nb, and $TiO_2$:F are all anisotropic, where the $m_n^*$ along the $a(b)$-axis is about 7–8 times larger than the value along the $c$-axis. The result of $TiO_2$:Nb is consistent well with the results of Hirose and his coworkers [31], who reported $m_n^*$ along the $a$- and the $c$-axis as ~0.6 $m_0$ and ~3.3 $m_0$, respectively, via Drude analysis. By comparing, $TiO_2$:Nb has a very similar $m_n^*$ with undoped $TiO_2$ along the $a(b)$ axis, and a little lower along the $c$-axis. The values of $m_n^*$ for $TiO_2$:F, however, compared with $TiO_2$:Nb, increase along the $a(b)$- and the $c$-axis by 16.98% and 4.38%, respectively. Therefore, in contrast with $TiO_2$:Nb, the poorer electron mobility of $TiO_2$:F is predictable because the larger effective mass is supposedly negative to the electron mobility.

The contour plots of charge density for undoped $TiO_2$, $TiO_2$:Nb and $TiO_2$:F are shown in Fig. 3. The overlap contours between Ti (Nb) and O (F) atoms reveal the well-known effect of a covalent bond that charges move to the interatomic sites to screen the ionic Coulomb repulsions. By comparing, the charge density around Ti and Nb in both undoped $TiO_2$ and Nb doped $TiO_2$ coincides well with each other. This correlation explains the high solubility of Nb, which can be up to ~40% in the experiment [32]. The charge density between the Ti and F atoms in $TiO_2$:F, however, is much less, implying that Ti–F bonding is more ionic, which can be attributed to the higher electro-negativity of the F atom compared with the O atom.

To further quantitatively investigate charge transfers, the charges of Ti, Nb, O, and F in undoped $TiO_2$, $TiO_2$:Nb, and $TiO_2$:F were calculated by using the Mulliken population method [33], the results of which are shown in Table 2. Since Mulliken populations are very basis-dependent and their absolute value is physically meaningless, hence, only deviations from the corresponding elementary substance values are listed. The atomic charges of Ti and O atoms in undoped $TiO_2$ are +1.27 and −0.63, respectively. Both deviate from the nominal value expected in a purely ionic state (Ti: +4; O: −2). This deviation partially reflects the covalent character of the bonds between Ti and O, which is in good agreement with the contour plots in Fig. 3. After doping, the charges of Ti and O atoms change to +1.26 and −0.64, respectively, for both $TiO_2$:Nb and $TiO_2$:F. This change indicates that the extra electron from the doping atom (Nb or F) influences the occupation states of the Ti 3d and O 2p orbits. The charge of Nb is +1.58, 0.32 larger than that of Ti in $TiO_2$:Nb. The discrepancy reflects that Nb releases 0.32 more electrons into the conduction. In $TiO_2$:F, the atomic charge of F is

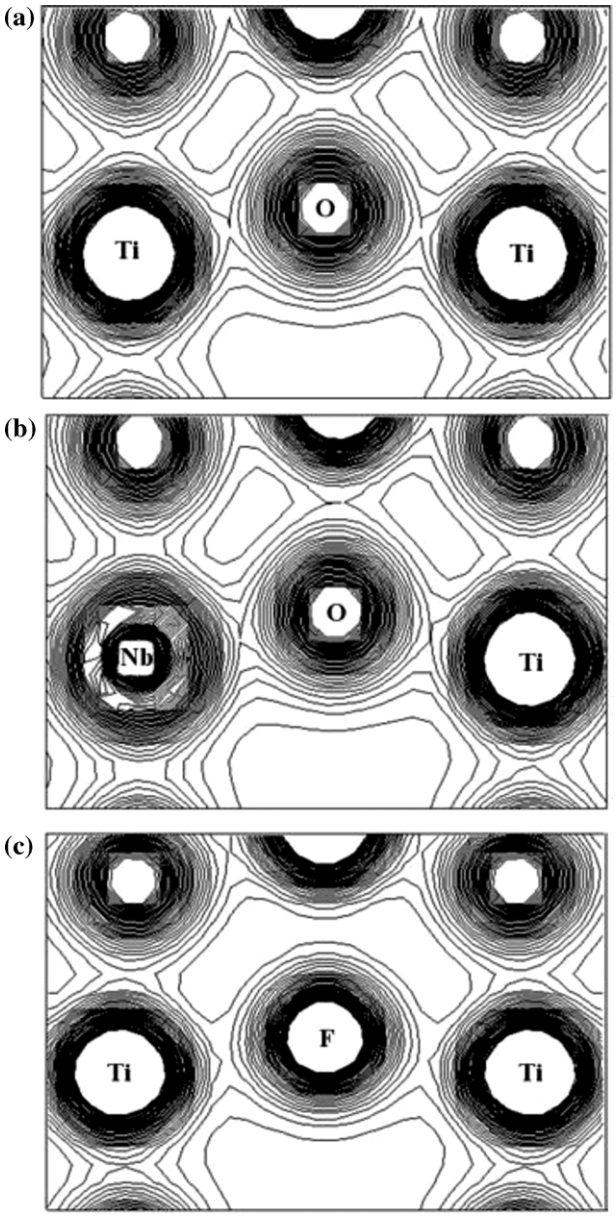


**Fig. 3.** Contour charge density for (a) undoped $TiO_2$, (b) $TiO_2$:Nb and (c) $TiO_2$:F on the (0 1 0) surface (contour line interval is 0.1 e/Å$^3$).

−0.46, 0.18 larger than that of O, which is also indicative of the release of 0.18 more electrons into the conduction band by F. However, this number is only almost half the value in the condition of $TiO_2$:Nb. As a result, $TiO_2$:Nb can be expected to create more carriers compared with $TiO_2$:F. The experimental ionization efficiency of Nb in $TiO_2$:Nb is >90% and the carriers density is around $10^{21}$ cm$^{-3}$ [34,35]. Although there is no available experimental ionization efficiency of F in $TiO_2$:F, the value is expected to be much lower, and poor carrier density in $TiO_2$:F will not be hard to predict.

**Table 2**
Mulliken charges for undoped $TiO_2$, $TiO_2$:Nb and $TiO_2$:F.

| | Ti | O | Nb | F |
|---|---|---|---|---|
| Undoped $TiO_2$ | +1.27 | −0.63 | | |
| $TiO_2$:Nb | +1.26 | −0.64 | +1.58 | |
| $TiO_2$:F | +1.26 | −0.64 | | −0.46 |

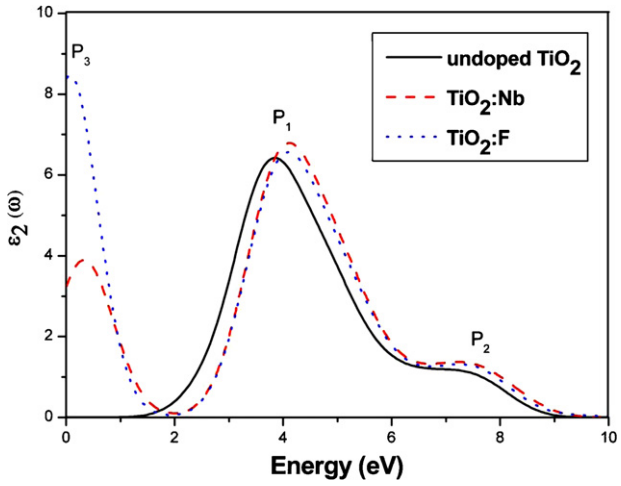


**Fig. 4.** Imaginary part of dielectric constant $\varepsilon_2(\omega)$ for undoped $TiO_2$, $TiO_2$:Nb and $TiO_2$:F.

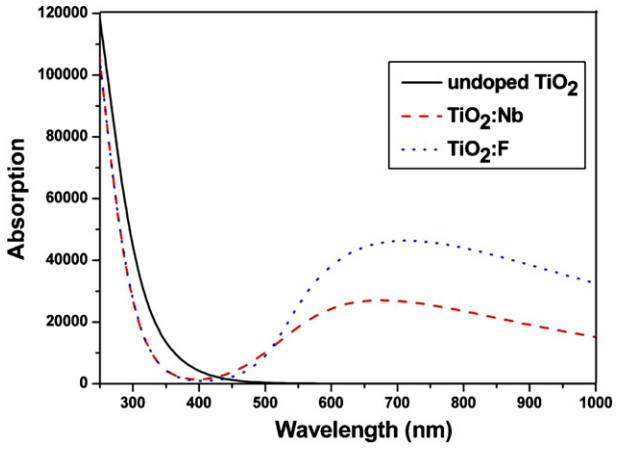


**Fig. 5.** Optical absorption spectra of undoped $TiO_2$, $TiO_2$:Nb and $TiO_2$:F.

### 3.2. Optical properties

To investigate the optical properties of a material, it is necessary to study the complex dielectric function,

$$\varepsilon(\omega) = \varepsilon_1(\omega) + i\varepsilon_2(\omega) \quad (2)$$

which is mainly related to the electronic structure of a compound. Other optical constants, such as the refractive index $n(\omega)$, extinction coefficient $k(\omega)$, optical reflectivity $R(\omega)$, absorption coefficient $\alpha(\omega)$, energy-loss spectrum $L(\omega)$, and complex conductivity function $\sigma(\omega)$, can be gained from the complex dielectric function $\varepsilon(\omega)$. The real part of the complex dielectric function $\varepsilon_1(\omega)$ can also be evaluated from the imaginary part $\varepsilon_2(\omega)$ through the famous Kramers–Kronig relationship [36–38]. Thus, we mainly pay attention to the imaginary part of the complex dielectric function $\varepsilon_2(\omega)$.

The calculated $\varepsilon_2(\omega)$ values for undoped $TiO_2$, $TiO_2$:Nb, and $TiO_2$:F are shown in Fig. 4. The undoped $TiO_2$ clearly shows two peaks. The peak at about 3.84 eV, named $P_1$, mainly comes from the electron transition between O 2p in the highest valence band and Ti 3d in the lowest conduction band; the broader peak at about 7 eV, named $P_2$, mainly comes from the transition between the deeper valance band and the conduction band. After the doping of Nb and F, $P_1$ shifts to higher energy at approximately 4.13 and 4.10 eV, respectively. The shift to a higher energy corresponds to the widen band gap after doping, as well as the influence of the Burstein-moss effect mentioned above. The little change in the position of $P_2$ indicates that the effect of dopants on the band structure is mainly around the highest valence band and the lowest conduction band. The calculated $\varepsilon_2(\omega)$ of $TiO_2$:Nb and $TiO_2$:F around $P_1$ and $P_2$ are almost identical, which result from the similar band structure they have. The major difference of $\varepsilon_2(\omega)$ between undoped and doped $TiO_2$ is a new peak at a lower energy around 0.5 eV, named $P_3$, found in both Nb- and F-doped $TiO_2$. These peaks can be attributed to the electron transition from the occupied Ti 3d orbits near the Fermi level to the higher unoccupied orbits. The value of $P_3$ for $TiO_2$:F is much larger than that for $TiO_2$:Nb, which indicates that the interaction between photons and electrons in $TiO_2$:F in the low energy region is much stronger. This may lead into more intensive absorption in $TiO_2$:F than in $TiO_2$:Nb in the visible and near-infrared regions.

In order to make the absorptions more clear, the absorptions of $TiO_2$:Nb and $TiO_2$:F were also calculated as shown in Fig. 5. Due to underestimation of the band gap, attaining the exact optical band gap is difficult. To overcome such a discrepancy, we use the energy scissors with a value of 1.13 eV for calculating the absorption [39], which is equal to the difference between the theoretical and experimental gap values of undoped anatase $TiO_2$. It is clearly observed that both Nb- and F-doping induce increased optical absorption in the visible and near-infrared regions. And in that regions, the absorption in $TiO_2$:F is ~2 times larger than that in $TiO_2$:Nb, which is in good agreement with the $\varepsilon_2(\omega)$ of $P_3$ in Fig. 4. It is worth mentioning that the shapes of absorption curve calculated here consist well with the experimental results that there is a distinct absorption peak in the visible and near infrared regions both for Nb and F doped $TiO_2$ [40,41]. Kurita et al. [40] also attributed the phenomena to the free electrons induced by the dopants. These results imply that $TiO_2$:F is more suitable for being used as a photocatalytic material rather than as a TCO.

## 4. Conclusions

The electronic and optical properties of Nb- and F- doped anatase $TiO_2$ were calculated through the first-principles method, with the corresponding properties of undoped anatase $TiO_2$ as a reference. Comparing with $TiO_2$:Nb, the effective mass of $TiO_2$:F increased by 16.98% and 4.38% along the *a*-axis and *c*-axis, respectively. This increase indicates the poorer electronic mobility of $TiO_2$:F. The dopant Nb released 0.32 more electrons than Ti, which is almost twice the number in the condition of $TiO_2$:F. The release of less electrons implies that the carrier density in $TiO_2$:F will be much lower than that in $TiO_2$:Nb. In terms of optical properties, the interaction between photons and electrons in $TiO_2$:F is much stronger, which increases photon absorption and lowers transparency, especially in the visible and near-infrared regions. All the electronic and optical properties suggest that $TiO_2$:F is much less suitable than $TiO_2$:Nb for being utilized as a TCO material.

## Acknowledgments

This work is financially supported by the National Natural Science Foundation of China (no. 51002135) and the Ph.D. Programs Foundation of Ministry of Education of China (20100101120105). The authors would like to thank the Zhejiang University National Science Park for providing computational support during the period of this research.

## References

[1] A.L. Dawar, J.C. Joshi, J. Mater. Sci. 19 (1984) 1–23.
[2] D.S. Ginley, C. Bright, Mater. Res. Bull. 25 (2000) 15–18.
[3] C.A. Hoel, T.O. Mason, J.F. Gaillard, K.R. Poeppelmeier, Chem. Mater. 22 (2010) 3569–3579.
[4] T. Minami, Thin Solid Films 516 (2008) 5822–5828.

[5] M. Benhaliliba, C.E. Benouis, M.S. Aida, A.S. Juarez, F. Yakkuphanoglu, A.T. Silver, J. Alloys Compd. 506 (2010) 548–553.
[6] Y. Furubayashi, T. Hitosugi, Y. Yamamoto, K. Inaba, G. Kinoda, Y. Hasegawa, Appl. Phys. Lett. 86 (2005) 252101.
[7] G.Q. Wang, W. Lan, G.J. Han, Y. Wang, Q. Su, X.Q. Liu, J. Alloys Compd. 509 (2011) 4150–4153.
[8] T. Hitosugi, Y. Furubayashi, A. Ueda, K. Itabashi, K. Inaba, Y. Hirose, G. Kinoda, Y. Yamamoto, T. Shimada, T. Hasegawa, Jpn. J. Appl. Phys. 44 (2005) L11063.
[9] U. Takeuchi, A. Chikamatsu, T. Hitosugi, H. Kumigashira, M. Oshima, Y. Hirose, T. Shimada, T. Hasegawa, J. Appl. Phys. 107 (2010) 023705.
[10] D.M. Chen, G. Xu, L. Miao, L.H. Chen, S. Nakao, P. Jin, J. Appl. Phys. 107 (2010) 063707.
[11] T. Hitosugi, N. Yamada, S. Nakao, Y. Hirose, T. Hasegawa, Phys. Status Solidi A 207 (2010) 1529–1537.
[12] K. Lv, J.G. Yu, L.Z. Cui, S.L. Chen, M. Li, J. Alloys Compd. 509 (2011) 4557–4562.
[13] G.S. Wu, A.C. Chen, J. Photochem. Photobiol. A: Chem. 195 (2008) 47–53.
[14] J.J. Xu, Y.H. Ao, D.G. Fu, C.W. Yuan, Appl. Surf. Sci. 254 (2008) 3033–3038.
[15] J. He, Q.Z. Cai, Y.G. Ji, H.H. Luo, D.J. Li, B. Yu, J. Alloys Compd. 482 (2009) 476–481.
[16] M.L. Guo, X.D. Zhang, C.T. Liang, G.Z. Jia, Chin. Phys. Lett. 27 (2010) 057103.
[17] T. Hitosugi, H. Kamisaka, K. Yamashita, H. Nogawa, Y. Furubayashi, S. Nakao, N. Yamada, A. Chikamatsu, H. Kumigashira, M. Oshima, Y. Hirose, T. Shimada, T. Hasegawa, Appl. Phys. Express 1 (2008) 111203.
[18] X.D. Liu, E.Y. Jiang, Z.Q. Li, Q.G. Song, Appl. Phys. Lett. 92 (2008) 252104.
[19] H. Kamisaka, T. Hitosugi, T. Suenaga, T. Hasegawa, K. Yamashita, J. Chem. Phys. 131 (2009) 034702.
[20] H. Kamisaka, T. Suenaga, H. Nakamura, K. Yamashita, J. Phys. Chem. C 114 (2010) 12777–12783.
[21] M.D. Segall, P.J.D. Lindan, M.J. Probert, C.J. Pickard, P.J. Hasnip, S.J. Clark, M.C. Payne, J. Phys.:Condens. Matter 14 (2002) 2717–2744.
[22] M.C. Payne, M.P. Teter, D.C. Allan, T.A. Arias, J.D. Joannopoulos, Rev. Mod. Phys. 64 (1992) 1045–1097.
[23] J.P. Perdew, K. Burke, M. Ernzerhof, Phys. Rev. Lett. 77 (1996) 3865–3868.
[24] J. Sun, X.F. Zhou, Y.X. Fan, J. Chen, H.T. Wang, X. Guo, J. He, Y. Tian, Phys. Rev. B 73 (2006) 045108.
[25] H.J. Monkhorst, J.D. Pack, Phys. Rev. B 13 (1976) 5188–5192.
[26] E. Burstein, Phys. Rev. 93 (1954) 632–633.
[27] T.S. Moss, Proc. Phys. Soc. Lond. B 67 (1954) 775–782.
[28] A.V. Emeline, Y. Furubayashi, X.T. Zhang, M. Jin, T. Murakami, A. Fujishima, J. Phys. Chem. B 109 (2005) 24441–24444.
[29] H. Tang, H. Berger, P.E. Schmid, F. Lévy, Solid State Commun. 92 (1994) 267–271.
[30] J.P. Perdew, M. Levy, Phys. Rev. Lett. 51 (1983) 1884–1887.
[31] Y. Hirose, N. Yamada, S. Nakao, T. Hitosugi, T. Shimada, T. Hasegawa, Phys. Rev. B 79 (2009) 165108.
[32] L. Sheppard, T. Bak, J. Nowotny, C.C. Sorrell, S. Kumar, A.R. Gerson, M.C. Barnes, C. Ball, Thin Solid Films 510 (2006) 119–124.
[33] R.S. Mulliken, J. Chem. Phys. 23 (1955) 1833–1840.
[34] Y. Furubayashi, T. Hitosugi, Y. Yamamoto, Y. Hirose, G. Kinoda, K. Inaba, T. Shimada, T. Hasegawa, Thin Solid Films 496 (2006) 157–159.
[35] T. Hitosugi, N. Yamada, N.L.H. Hoang, J. Kasai, S. Nakao, T. Shimada, T. Hasegawa, Thin Solid Films 517 (2009) 3106–3109.
[36] C. Ambrosch-Draxl, J.O. Sofo, Comput. Phys. Commun. 175 (2006) 1–14.
[37] X.Y. Yu, C.S. Li, Y. Ling, T.A. Tang, Q. Wu, J. Kong, J. Alloys Compd. 507 (2010) 33–37.
[38] H. Wang, Y. Chen, Y. Kaneta, S. Iwata, J. Alloys Compd. 491 (2010) 550–559.
[39] F.M. Hossain, L. Sheppard, J. Nowotny, G.E. Murch, J. Phys. Chem. Solids 69 (2008) 1820–1828.
[40] D. Kurita, S. Ohta, K. Sugiura, H. Ohta, K. Koumoto, J. Appl. Phys. 100 (2006) 096105.
[41] G.D. Yang, Z. Jiang, H.H. Shi, M.O. Jones, T.C. Xiao, P.P. Edwards, Z.F. Yan, Appl. Catal. B-Environ. 96 (2010) 458–465.